Check for updates

Behavior of H_2O surrounding NH_4^+ and Al^{3+} in $NH_4Al(SO_4)_2 \cdot 12H_2O$ by ^1H MAS NMR, ^{14}N NMR, and ^{27}Al NMR

Ae Ran Lim [ID] *[ab]

In order to understand the thermodynamic properties and structural geometry of $NH_4Al(SO_4)_2 \cdot 12H_2O$, we studied the magic angle spinning nuclear magnetic resonance (MAS NMR) and static NMR as a function of temperature. The changes of the chemical shifts, linewidths, resonance frequencies, and spin–lattice relaxation times for ^1H, ^{14}N, and ^{27}Al nuclei near T_d (=335 K), which is interpreted as the onset of partial thermal decomposition, are due to the structural phase transition. The changes near T_d are related to the loss of H_2O, which probably disrupts the forms of the octahedra of water molecules surrounding NH_4^+ and Al^{3+} ions. This mechanism above T_d is related to hydrogen-bond transfer involving the breakage of the weak part of the hydrogen bond.

I. Introduction

The alums can be represented by the general formula $A^IB^{III}(SO_4)_2 \cdot 12H_2O$, where A is a monovalent cation such as Na, K, Rb, Cs, or NH_4, and B is a trivalent cation such as Al, Fe, or Cr.[1–11] It is well known that there are a considerable number of alums $A^IB^{III}(SO_4)_2 \cdot 12H_2O$ that exhibit ferroelectric activity.[12] The twelve water molecules are located in an octahedral coordination in two crystallographically-different areas surrounding the A^I cation and the B^{III} ion complex. A complex network of H-bonds is one of the main features of alum structures. Current interest in these compounds lies in the fact that a number of them, particularly when A^I is NH_4, are ferroelectric at low temperature. $NH_4Al(SO_4)_2 \cdot 12H_2O$ crystals, one of the $A^IB^{III}(SO_4)_2 \cdot 12H_2O$ types, have a cubic structure and belong to the space group $Pa\bar{3}$ with $Z = 4$ per unit cell at room temperature. The lattice constants of $NH_4Al(SO_4)_2 \cdot 12H_2O$ crystals are $a = b = c = 12.242$ Å.[13] The NH_4^+ and Al^{3+} ions in the $NH_4Al(SO_4)_2 \cdot 12H_2O$ crystal are each surrounded by six water molecules, as shown in Fig. 1. As in other alums, each trivalent Al^{3+} is surrounded by an almost regular octahedron of six water molecules, whereas the remaining six water molecules surrounding the NH_4^+ cation form a highly distorted octahedron. In the case of $NH_4Al(SO_4)_2 \cdot 12H_2O$, the bond-length of $Al–6H_2O$ is 1.916 Å and the bond-length of $NH_4–6H_2O$ has a mean value of 3.051 Å.[14]

The phase transition temperature of $NH_4Al(SO_4)_2 \cdot 12H_2O$ crystals at low temperature has been reported to be 58 K and 71 K on cooling and heating, respectively.[9,13] According to previous reports, $NH_4Al(SO_4)_2 \cdot 12H_2O$ melts congruently at 367.13 K with a phase transition enthalpy of 122.2 kJ mol^{-1}.[11] In addition, the phase transition temperatures were reported as 370 K, 390 K, and 495 K using differential scanning calorimetry (DSC) by our group.[15] Furthermore, the mass loss begins in the vicinity of 335 K ($=T_d$), which is interpreted as the onset of partial thermal decomposition. On the other hand, the quadrupole coupling constants for ^{14}N and ^{27}Al in $NH_4Al(SO_4)_2 \cdot 12H_2O$ crystals have been reported to be 202 kHz and 446 kHz at room temperature, respectively.[16–19] The ^1H spin–lattice relaxation time T_1 in the laboratory frame and spin–lattice relaxation time $T_{1\rho}$ in the rotating frame of $NH_4Al(SO_4)_2 \cdot 12H_2O$ below 200 K have been studied by Svare *et al.*,[20] and were explained in terms of the hopping of NH_4^+ between two positions with different orientations and electron dipole moments.[19] In addition, the nuclear magnetic resonance (NMR) spectrum and the spin–lattice relaxation times in the laboratory frame for ^1H and ^{27}Al of $NH_4Al(SO_4)_2 \cdot 12H_2O$ crystals above 180 K were previously reported; the changes in the temperature dependences of the relaxation times near T_d were related to the loss of H_2O, which probably disrupts the forms of the octahedral of water molecules surrounding Al^{3+}.[15] Although these interesting properties have been studied by many methods, those related to the thermodynamic properties at high temperature have not yet been reported.

In the present study, the chemical shift, linewidth, and spin–lattice relaxation time, $T_{1\rho}$, in the rotating frame of $NH_4Al(SO_4)_2 \cdot 12H_2O$ were measured as a function of temperature using ^1H magic angle spinning (MAS) NMR, focusing on the role of NH_4 and H_2O. In addition, the ^{14}N NMR spectra in $NH_4Al(SO_4)_2 \cdot 12H_2O$ single crystals as a function of temperature were discussed in order to elucidate the structural geometry. At high temperature, we use these results to analyze the behavior of NH_4^+ and Al^{3+} surrounded by six water molecules,

ᵃAnalytical Laboratory of Advanced Ferroelectric Crystals, Jeonju University, Jeonju 55069, Korea

ᵇDepartment of Science Education, Jeonju University, Jeonju 55069, Korea. E-mail: aeranlim@hanmail.net; arlim@jj.ac.kr
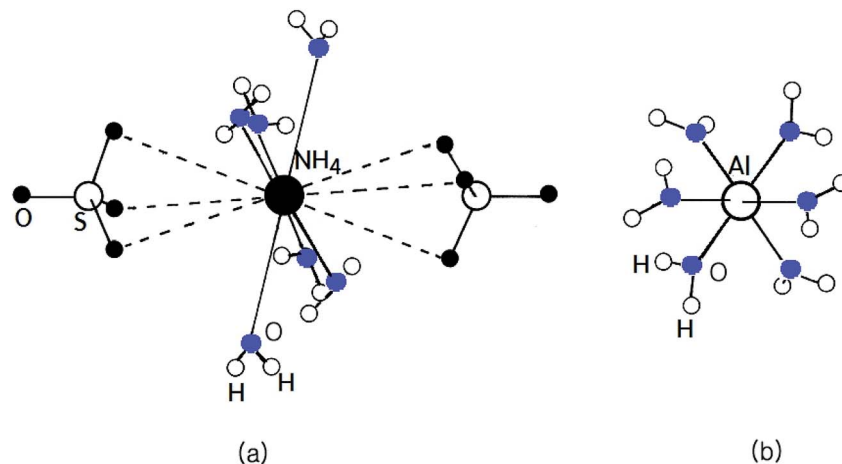
Fig. 1 The cubic structure of $NH_4Al(SO_4)_2 \cdot 12H_2O$ single crystals at room temperature. (a) Six water molecules surrounding NH_4^+ and (b) six water molecules surrounding Al^{3+}.

respectively, from the results of ^1H MAS NMR, ^{14}N NMR here obtained, and the ^{27}Al NMR previously reported. The connection between the crystal structure and the thermal properties of $NH_4Al(SO_4)_2 \cdot 12H_2O$ is discussed.

II. Experimental procedure

Single crystals of $NH_4Al(SO_4)_2 \cdot 12H_2O$ were prepared by the slow evaporation of an aqueous solution. The single crystals are transparent, colorless, and hexagonally-shaped.

^1H MAS NMR spectra and the spin–lattice relaxation time $T_{1\rho}$ in the rotating frame were obtained at the Larmor frequency of 400.13 MHz using a Bruker 400 MHz NMR spectrometer at the Korea Basic Science Institute, Western Seoul Center. Chemical shifts were referred with respect to tetramethylsilane (TMS). Powdered samples were placed in a 4 mm CP/MAS probe, and the MAS rate was set to 10 kHz for ^1H MAS measurement to minimize spinning sideband overlap. ^1H $T_{1\rho}$ values were determined using a $\pi/2$–t sequence by varying the duration of the spin-locking pulses. The widths of the $\pi/2$ pulses used for measuring the $T_{1\rho}$ values of ^1H were 3.6 μs below 340 K and 4.35 μs above 350 K.

In addition, the ^{14}N NMR spectra of the $NH_4Al(SO_4)_2 \cdot 12H_2O$ single crystals in the laboratory frame were measured using a Unity INOVA 600 NMR spectrometer at the Korea Basic Science Institute, Western Seoul Center. The static magnetic field was 14.1 T, and the Larmor frequency was set to $\omega_0/2\pi = 43.342$ MHz. The ^{14}N NMR experiments were performed using a solid-state echo sequence: 4.5 μs–t–4.5 μs–t. The temperature dependent NMR measurements were obtained over the temperature range 180–400 K. The samples were maintained at a constant temperature by controlling the nitrogen gas flow and the heater current.

III. Experimental results and discussion

A. ^1H MAS NMR

The ^1H MAS NMR spectrum in $NH_4Al(SO_4)_2 \cdot 12H_2O$ was measured as a function of temperature. The ^1H MAS NMR

spectra shows only one peak at a chemical shift of $\delta = 6.6$ ppm at room temperature, as shown in Fig. 2. There are ammonium protons and water protons of two kinds in the $NH_4Al(SO_4)_2 \cdot 12H_2O$ structure. In our experimental results, the proton signals due to the ammonium and water protons cannot be distinguished; the four ammonium protons and the twenty-four water protons should yield two superimposed lines with intensity in a theoretical ratio of 1 : 6. The signal due to the ammonium protons might include the signal due to the water protons with a broad linewidth. The abrupt change in the chemical shift near 335 K ($=T_d$), interpreted as the onset of partial thermal decomposition, may be due to the breaking of N–H bonds in NH_4 or loss of H_2O.

The full width at half maximum (FWHM) of the ^1H MAS NMR signal as a function of temperature is shown in the inset in Fig. 2. As the temperature increases, the FWHM near T_d decreases in a stepwise shape. This stepwise narrowing is generally caused by internal motions, which have a temperature
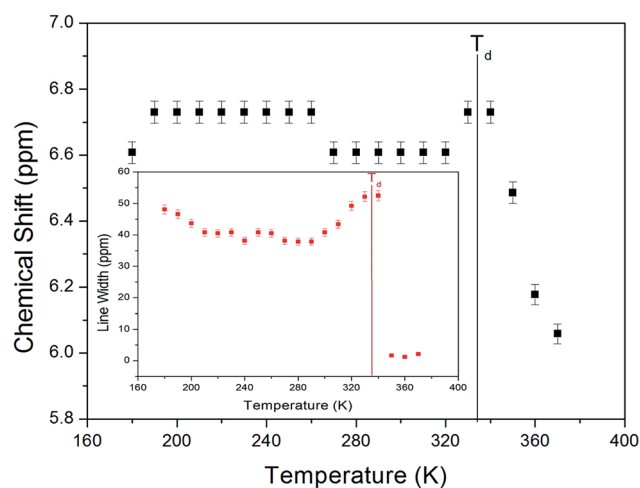

Fig. 2 Chemical shift of ^1H MAS NMR spectrum in $NH_4Al(SO_4)_2 \cdot 12H_2O$ as a function of temperature (inset: line width of ^1H MAS NMR spectrum in $NH_4Al(SO_4)_2 \cdot 12H_2O$ as a function of temperature).

dependence that is related to that observed for the chemical shift. The shape of the line abruptly changes with increasing temperature from the Gaussian shape of a rigid lattice to a Lorentzian shape. The linewidth below T_d is severely broadened because of the overlap of the ammonium protons and water protons. Above T_d, the linewidth undergoes an abrupt drop, and the linewidth becomes much narrower. This mechanism above T_d is related to hydrogen-bond transfer involving the breakage of the weak part of the hydrogen bond.

The recovery traces for the resonance line of ^1H in NH_4-$Al(SO_4)_2 \cdot 12H_2O$ are represented by a single exponential function of $M(t) = M(\infty)\exp(-t/T_{1\rho})$, where $M(t)$ is the magnetization as a function of the spin-locking pulse duration t, and $M(\infty)$ is the total nuclear magnetization of ^1H at thermal equilibrium.[21] Fig. 3 shows the recovery traces fitted with the single exponential function for delay times ranging from 0.001 ms to 70 ms at 200, 250, 300, and 360 K. The recovery traces for the ^1H nuclei vary with the delay time. These recovery traces also varied depending upon the temperature. From the slopes of the recovery traces, the ^1H spin–lattice relaxation time, $T_{1\rho}$, in the rotating frame is obtained in Fig. 4 as a function of inverse temperature. As for the chemical shift, the $T_{1\rho}$ values of ^1H are significantly different with the temperature. This indicates that the configuration of ^1H in the NH_4 and H_2O is strongly dependent on the temperature. The significant difference in the $T_{1\rho}$ values indicates that $NH_4Al(SO_4)_2 \cdot 12H_2O$ is strongly affected, which is mainly the result of structural changes involving water molecules. The proton $T_{1\rho}$ data show evidence of a change near T_d, which coincides with the measured changes in the ^1H chemical shift. The ^1H $T_{1\rho}$ values are strongly dependent the temperature, *i.e.*, distinct molecular motions are present as the temperature changes. Below T_d, the relaxation time undergoes two minimum of 1.81 ms at 230 K and 1.44 ms at 340 K, respectively.

The $T_{1\rho}$ values are related to the rotational correlation time τ_C, which directly measures the rate of molecular motion. The experimental value of $T_{1\rho}$ can be expressed in terms of τ_C using
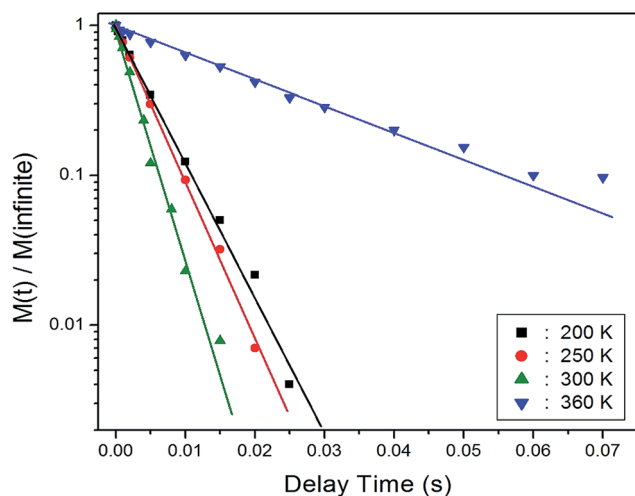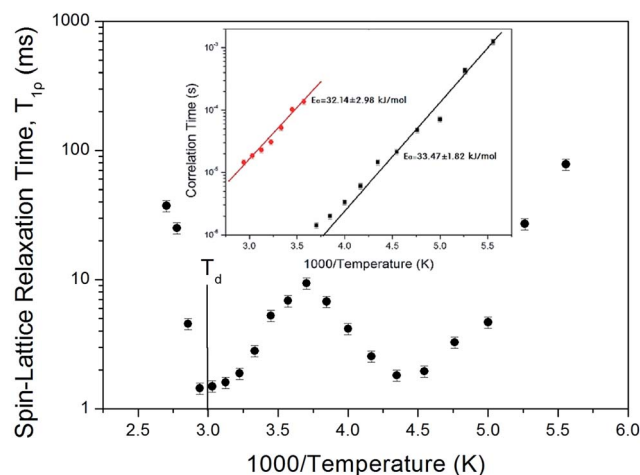

Fig. 4 Temperature dependence of the spin–lattice relaxation time $T_{1\rho}$ in the rotating frame of the ^1H nuclei in $NH_4Al(SO_4)_2 \cdot 12H_2O$ (inset: the correlation times for ^1H as a function of inverse temperature in $NH_4Al(SO_4)_2 \cdot 12H_2O$).

a molecular motion suggested by the Bloembergen–Purcell–Pound (BPP) theory. $T_{1\rho}$ for a spin–lattice interaction of molecular motion is given by[22–24]

$$T_{1\rho}^{-1} = (n/20)(\gamma_H\gamma_N\hbar/r_{H-N}^3)^2[4g(\omega_1) + g(\omega_H - \omega_N) + 3g(\omega_N) + 6g(\omega_H + \omega_N) + 6g(\omega_H)], \quad (1)$$

where,

$$g(\omega_1) = \tau_C/[1 + \omega_1^2\tau_C^2],$$

$$g(\omega_H - \omega_N) = \tau_C/[1 + (\omega_H - \omega_N)^2\tau_C^2],$$

$$g(\omega_N) = \tau_C/[1 + \omega_N^2\tau_C^2],$$

$$g(\omega_H + \omega_N) = \tau_C/[1 + (\omega_H + \omega_N)^2\tau_C^2], \text{ and}$$

$$g(\omega_H) = \tau_C/[1 + \omega_H^2\tau_C^2].$$

Here, γ_H and γ_N are the gyromagnetic ratios for the ^1H and ^{14}N nuclei, respectively, n is the number of directly bound protons, r_{H-N} is the H–N internuclear distance, $\hbar$ is the Planck constant, ω_H and ω_N are the Larmor frequencies of ^1H and ^{14}N, respectively, and ω_1 is the spin-lock field frequency of 69.44 kHz. Our data analysis assumed that $T_{1\rho}$ would show a minimum when $\omega_1\tau_C = 1$, and that the BPP relation between $T_{1\rho}$ and the characteristic frequency of ω_1 could be applied. Since $T_{1\rho}$ displayed two minimum in Fig. 4, it was possible to determine the coefficient in the BPP formula. This coefficient enabled us to calculate the parameter τ_C as a function of inverse temperature. The temperature dependence of τ_C follows a simple Arrhenius expression[21]

$$\tau_C = \tau_o \exp(-E_a/RT), \quad (2)$$

where τ_o is a pre-exponential factor, T is the temperature, R is the gas constant, and E_a is the activation energy. E_a for the tumbling motion can be calculated as the slope in the $\ln \tau_C$ *vs.*

Fig. 3 Recovery traces for ^1H nucleus as a function of the delay time at 200, 250, 300, and 360 K.

1000/T plot, which is shown inset in Fig. 4. For tumbling motion, we obtained the values $E_a = 33.47 \pm 1.82$ kJ mol^{-1} and $E_a = 32.14 \pm 2.98$ kJ mol^{-1} for the low- and high-temperature, respectively. These values are considered equal within the error range.

B. ^{14}N NMR

In order to obtain information concerning the possible distortion surrounded the ^{14}N ion, the NMR spectrum of ^{14}N ($I = 1$) was obtained using static NMR at a Larmor frequency of $\omega_0/2\pi = 43.342$ MHz, as a function of temperature. Two resonance lines were expected from the quadrupole interactions of the ^{14}N nucleus. The magnetic field was applied along the crystallographic axis. The *in situ* ^{14}N NMR spectra and the resonance frequency in $NH_4Al(SO_4)_2 \cdot 12H_2O$ single crystals are plotted in Fig. 5(a and b), as a function of temperature. The ^{14}N NMR spectra of the three groups of two resonance lines for ^{14}N are attributed to the NH_4. The lines represented by the same color indicate the same pairs for ^{14}N, as shown in Fig. 5(b). According to the crystallography results previously reported, the NH_4 tetrahedron appears to be slightly elongated along a 3-fold symmetry axis; the NH_4^+ ions have a longer N–H distance and shorter N–H distance.[25] The results of the three groups of ^{14}N show that the tetrahedral symmetry for NH_4^+ ion is not highly symmetric and that the stronger distortion of the crystallography is indicated. In addition, this splitting of the ^{14}N

(a)
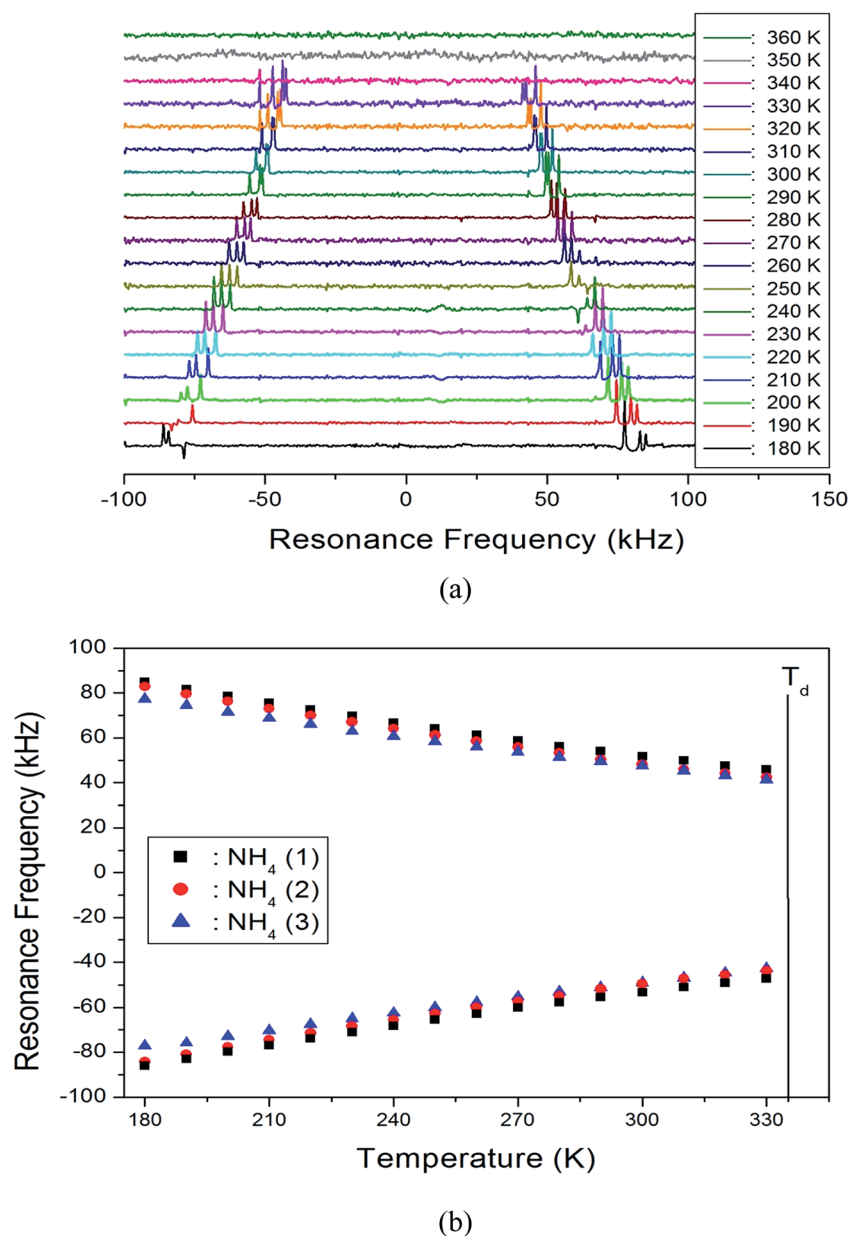

(b)

Fig. 5   (a) *In situ* ^{14}N NMR spectrum in $NH_4Al(SO_4)_2 \cdot 12H_2O$ single crystal as a function of temperature and (b) resonance frequency of ^{14}N NMR spectrum in $NH_4Al(SO_4)_2 \cdot 12H_2O$ single crystal as a function of temperature.

resonance lines slightly decreases with increasing temperature. Note that temperature-dependent changes in the ^{14}N resonance frequency are generally attributed to changes in the structural geometry, indicating a change in the quadrupole coupling constant of the ^{14}N nuclei. In addition, the ^{14}N signal near T_d disappears, and this phenomenon may be related to the ammonium ions dissociating.

C. ^{27}Al NMR

The NMR spectrum of ^{27}Al ($I = 5/2$) consists of a central line and four satellite resonance lines. The $NH_4Al(SO_4)_2 \cdot 12H_2O$ crystal structure is cubic, so a single resonance line is expected for the ^{27}Al nuclei. However, the NMR spectrum of ^{27}Al in NH_4-$Al(SO_4)_2 \cdot 12H_2O$ single crystals below T_d shows two groups of five resonance lines, as shown inset in Fig. 6. Moreover, only one ^{27}Al resonance line above T_d is obtained. The two types of magnetically inequivalent Al nuclei, Al(1) and Al(2), are present in the unit cell. Although the structure of the $NH_4Al(SO_4)_2$-$\cdot 12H_2O$ crystal is cubic, the environment of the Al sites surrounded by water molecules is not cubic; the water molecules surrounding Al^{3+} form a distorted octahedron. The presence of only one ^{27}Al resonance line near T_d is due to the structural phase transition. On the other hand, the temperature dependence of the resonance frequency of ^{14}N decreases with increasing temperature, whereas those of ^{27}Al have an opposite tendency to the usual decrease with increasing temperature.

The magnetization recovery of ^{27}Al does not follow a single exponential, but can be represented by a combination of three exponential functions:[15,26]

$$[M(\infty) - M(t)]/M(\infty) = 0.06 \exp(-0.8W_1t) \\ - 0.85 \exp(-1.5W_1t) - 0.09 \exp(-0.33W_1t), \quad (3)$$

where W_1 denotes the ^{27}Al spin–lattice transition rate corresponding to the $\Delta m = \pm 1$ transitions when $W_1 = W_2$. $M(t)$ is the nuclear magnetization at time t after saturation and the spin–lattice relaxation time, T_1, is the inverse W_1.

The ^{27}Al spin–lattice relaxation time, T_1, in the laboratory frame was measured in the temperature range of 180–420 K. The T_1 for ^{27}Al in this single crystal show very strong temperature dependences, as shown in Fig. 6. The T_1 for the Al(1) and Al(2) sites cannot be distinguished because of the overlap of the two central resonance lines for the Al(1) and Al(2) nuclei. T_1 near T_d is an abrupt drop, and T_1 above T_d is nearly constant with temperature. The change in the temperature dependence of T_1 near T_d is related to the beginning of the loss of H_2O. This drop is related to the loss of H_2O, and the forms of the octahedra of water molecules surrounding Al^{3+} are probably disrupted by the loss of H_2O.

IV. Conclusion

The thermodynamic properties and structural geometry of $NH_4Al(SO_4)_2 \cdot 12H_2O$ focusing on the role of NH_4 and H_2O, were investigated by ^1H MAS NMR, static ^{14}N NMR, and ^{27}Al NMR as a function of temperature. The changes in the temperature dependences of chemical shifts, line widths, spin–lattice relaxation times, and resonance frequency near T_d are related to changes in the symmetry of the octahedra of water molecules about NH_4^+ and Al^{3+}; these changes are related to the loss of H_2O, which probably disrupts the forms of the octahedra of water molecules surrounding NH_4^+ and Al^{3+}. The structural changes due to the loss of H_2O are significant at T_d, and the transformation at T_d is due to the breaking of hydrogen bonds. This mechanism above T_d is related to hydrogen-bond transfer involving the breakage of the weak part of the hydrogen bond.

Conflicts of interest

There are no conflicts to declare.

Acknowledgements

References

1 V. K. Sabirov, *J. Struct. Chem.*, 2015, **56**, 698.
2 S. You, Y. Zhang and Y. Zang, *J. Cryst. Growth*, 2015, **411**, 24.
3 C. L. Chang, S.-Y. Jeong and Y. K. Paik, *J. Appl. Phys.*, 2013, **113**, 17E105.
4 C. L. Chang, S.-Y. Jeong and Y. K. Paik, *Appl. Magn. Reson.*, 2013, **44**, 1245.
5 N. Kubota and M. Onosawa, *J. Cryst. Growth*, 2009, **311**, 4525.
6 M. Boujelben, M. Toumi and T. Mhiri, *Ann. Chimie Sci. Matériaux*, 2008, **33**, 379.
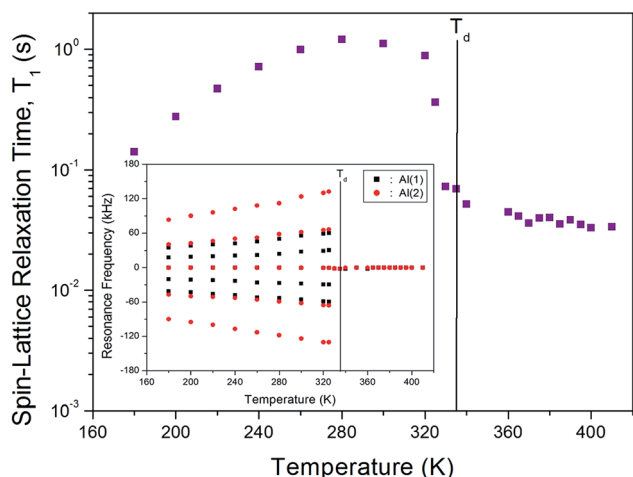7 Y. M. Korchak, V. B. Kapustyanyk, M. V. Partyka and V. P. Rudyk, *J. Appl. Spectrosc.*, 2007, **74**, 289.

Fig. 6 Temperature dependence of the spin–lattice relaxation time T_1 in the laboratory frame of the ^{27}Al nuclei in $NH_4Al(SO_4)_2 \cdot 12H_2O$ single crystal (inset: the resonance frequency of ^{27}Al NMR spectrum in $NH_4Al(SO_4)_2 \cdot 12H_2O$ single crystal as a function of temperature).

8 B. Pacewska and J. Pysiak, *J. Therm. Anal.*, 1991, **37**, 1389.

9 R. Bohmer, P. Lunkenheimer, J. K. Vij and I. Svare, *J. Phys.: Condens. Matter*, 1990, **2**, 5433.

10 S. Radhakrishna, B. V. R. Chowdari and A. K. Viswanath, *J. Chem. Phys.*, 1977, **66**, 2009.

11 F. Gronvold and K. K. Meisingset, *J. Chem. Thermodyn.*, 1982, **14**, 1083.

12 A. Sekine, M. Sumita, T. Osaka and Y. Makita, *J. Phys. Soc. Jpn.*, 1988, **57**, 4004.

13 A. M. Abdeen, G. Will, W. Schafer, A. Kirfel, M. O. Bargouth and K. Recker, *Z. Kristallogr.*, 1981, **157**, 147.

14 A. C. Larson and D. T. Cromer, *Acta Crystallogr.*, 1967, **22**, 793.

15 A. R. Lim, H.-G. Moon and J.-H. Chang, *Chem. Phys.*, 2010, **371**, 91.

16 W. G. Segleken and H. C. Torrey, *Phys. Rev.*, 1973, **38**, 1255.

17 N. Weiden and A. Weiss, *Berichte der Bunsengesellschaft für physikalische Chemie*, 1974, **78**, 1031.

18 W. C. Bailey and H. C. Story, *J. Chem. Phys.*, 1974, **60**, 1952.

19 S. Sinha and R. Srinivasan, *Pramana*, 1984, **22**, 345.

20 I. Svare and R. M. Holt, *Solid State Commun.*, 1979, **29**, 851.

21 A. Abragam, *The Principles of Nuclear Magnetism*, Oxford University Press, 1961.

22 J. L. Koenig, *Spectroscopy of Polymers*, Elsevier, New York, 1999.

23 A. R. Lim, *AIP Adv.*, 2016, **6**, 35307.

24 A. R. Lim, *J. Mol. Struct.*, 2017, **1146**, 324.

25 D. T. Cromer and M. I. Kay, *Acta Crystallogr.*, 1967, **22**, 800.

26 E. R. Andrew and D. T. Tunstall, *Proc. Phys. Soc., London*, 1961, **78**, 1.